Ethylene Decomposition on Rh(100): Theory and Experiment†

Davy L. S. Nieskens,* A. P. van Bavel, D. Curulla Ferre, and J. W. Niemantsverdriet

Schuit Institute of Catalysis, Eindhoven University of Technology, P.O. Box 513, 5600 MB Eindhoven, The Netherlands

Received: February 17, 2004; In Final Form: June 8, 2004

The decomposition of ethylene on a Rh(100) single crystal has been studied by a combination of experimental techniques: static secondary ion mass spectrometry (SSIMS), temperature-programmed desorption (TPD), low-energy electron diffraction (LEED), and high-resolution electron energy loss spectroscopy (HREELS), to gain insight into the nature of the reaction intermediates during the decomposition process. These experimental techniques were combined with a computational approach using density functional theory (DFT). Ethylene adsorbs irreversibly on the Rh(100) surface and eventually decomposes to atomic carbon and gas phase hydrogen. The type of intermediate species depends strongly on the initial surface coverage of ethylene. At low coverage, ethynyl (CCH) is the main intermediate species, whereas at high coverage a mixture of ethynyl, acetylene (CHCH), and ethylidyne (CCH_3) forms. The rate of decomposition is significantly slower at higher coverages, indicative of lateral interactions between coadsorbed species and site-blocking effects.

1. Introduction

The decomposition of olefins such as ethylene and propylene has been studied on many metals such as platinum, rhodium, palladium, and ruthenium.[1−5] Most of these studies were carried out on the fcc (111) or hcp (0001) surfaces, and there is less data available for the behavior of hydrocarbons on the more reactive fcc (100) surfaces. On the (111) surfaces ethylene decomposes at relatively low temperatures (typically room temperature) to either acetylene (CHCH) or ethylidyne (CCH_3). At higher temperatures, these species decompose further into ethynyl (CCH) and finally carbon. Relatively few papers address the decomposition of olefins on the more reactive (100) surfaces.[6−15]

Insight into the nature of the intermediate hydrocarbon fragments is important when investigating surface reactions of these hydrocarbon species with other species, like N-atoms. These reactions can lead to the formation of products with C−N bonds. For example, Van Hardeveld and co-workers[16−18] showed that all N-atoms coadsorbed to CH species on a Rh(111) surface reacted to HCN at temperatures that are substantially below those employed in industrial HCN synthesis. We are currently exploring similar reactions between hydrocarbon species that are larger than CH, on a range of surfaces, including Rh(100). For this study we need an adequate characterization of hydrocarbon species that occur on these surfaces. Hence, the purpose of this paper is to investigate which species appear during the decomposition of ethylene on the Rh(100) surface.

Ethylene adsorbs molecularly on this surface below 100 K, and upon increasing the temperature it fully decomposes into carbon and hydrogen. During the decomposition process, a number of species are present on the surface. In general, surfaces with square symmetry favor formation of species such as vinyl ($CHCH_2$), vinylidene (CCH_2), acetylene (CHCH), and ethynyl (CCH). Ethylidyne (CCH_3), which is a common intermediate on the (111) surfaces of many metals,[3,19−21] is usually not present on the (100) surfaces, however, apparently with the exception of rhodium, according to Slavin et al.[6,7] In this paper we investigate the decomposition of ethylene on Rh(100) by static secondary ion mass spectrometry (SSIMS), temperature-programmed desorption (TPD), low-energy electron diffraction (LEED), and high-resolution electron energy loss spectroscopy (HREELS). We combine the experimental techniques with a computational approach using density functional theory (DFT) calculations to determine the relative stabilities of each of the decomposition fragments. We show that the nature of the reaction intermediates depends strongly on the initial surface coverage of ethylene. For low initial ethylene coverages, ethynyl (CCH) is the main intermediate, while for high initial ethylene coverages a mixture of ethynyl, acetylene, and ethylidyne is observed.

2. Experimental Methods and Theoretical Details

TPD, LEED, and static SIMS experiments were carried out in a stainless steel ultrahigh vacuum (UHV) system with a base pressure of 1×10^{-10} mbar. Static SIMS spectra were taken by using a defocused 5 keV Ar^+ primary ion beam with a current density of 1 nA/cm^2 at an incident polar angle of 60° with respect to the surface normal. Secondary ions were collected under a polar angle of 30°. These conditions enable measurements in static mode, with a removal rate of less than one monolayer of adsorbates per several hours. A typical temperature-programmed experiment lasted 3 min at most. The HREELS experiments were carried out in a separate UHV system with a base pressure of 5×10^{-11} mbar (see Linke et al.[22] for further details). The HREELS spectra were recorded at 100 K and measured in specular scattering geometry (around 65°) with a typical resolution (elastic peak at full width at half-maximum) between 25 and 30 cm^{-1} (3.1−3.7 meV). The primary energy used was around 6 eV. Reported primary energies are not corrected for contact potential differences. In both setups, a rhodium single crystal of (100) orientation with a thickness of 1.2 mm was mounted on a movable sample rod

† Part of the special issue "Gerhard Ertl Festschrift".

* Corresponding author. Phone: +31-40-2474658. Fax: +31-40-2473481. E-mail: d.l.s.nieskens@tue.nl.

10.1021/jp049279m CCC: $27.50
Published on Web 08/04/2004

by two tantalum wires of 0.3 mm diameter, pressed into small grooves on the side of the crystal. This construction allows for resistive heating to 1500 K. The sample could be cooled to 88 K by flowing liquid nitrogen through the manipulator. Temperatures were measured using a chromel−alumel thermocouple spot-welded to the back of the crystal. For a general introduction into the techniques used here, we refer to Niemantsverdriet.[23]

The crystal surface was cleaned by cycles of argon sputtering and annealing under oxygen. Argon sputtering (0.5 keV, 6 μA/cm^2) at 920 K was used to remove small amounts of impurities, such as boron, sulfur, phosphorus, and chlorine, until these were no longer detectable with SIMS. Carbon appeared to be the most difficult impurity to remove, since it is known to dissolve into the bulk at elevated temperatures (>700 K)[24] and reappear after cooling the crystal. Near-surface carbon was removed by heating the crystal in 2×10^{-7} mbar O_2, cycling the temperature between 900 and 1100 K. Oxygen was removed, and surface ordering was restored by flashing the crystal to 1400 K. After flashing the crystal, a small amount of O_2 was adsorbed at low temperature, and the crystal was heated to 900 K. This was done to remove small amounts of carbon that had diffused to the surface during the flashing and subsequent cooling. Finally CO was dosed at 550 K to react away the remaining oxygen on the surface, and a flash to 900 K removed the excess of CO. After this procedure the SIMS spectra of the crystal showed no contamination, and the LEED picture showed a sharp p(1 × 1) pattern. After each experiment the procedure mentioned above (except argon sputtering) was repeated to remove the carbon that was created during the ethylene decomposition process.

Ethylene (Hoek Loos, 99.8% pure) was used without further purification. Gas dosing for all experiments was done at 100 K or lower. All temperature-programmed experiments were done at a heating rate of 5 K/s.

In the density functional theory calculations we have modeled the Rh(100) surface within the slab model approximation using a four-metal layer slab model, describing a p(2 × 2) unit cell, and six vacuum layers. The relative positions of the atoms are those as in the bulk, with an optimized lattice parameter of 3.8543 Å (the experimental value is 3.8034).[25] We have used the Vienna ab initio simulation package (VASP),[26,27] which performs an iterative solution of the Kohn−Sham equations in a plane-wave basis set. Plane-waves with a kinetic energy below or equal to 300 eV have been included in the calculation. The exchange-correlation energy has been calculated within the generalized gradient approximation (GGA) using the form of the functional proposed by Perdew and Wang,[28,29] usually referred to as Perdew−Wang 91 (PW91). The electron−ion interactions are described by optimized ultrasoft pseudopotentials for C, H, and Rh.[30] The reciprocal space has been sampled with an (8 × 8 × 1) *k*-points grid automatically generated using the Monkhorst−Pack method.[31] For the calculation of the fractional occupancies, a broadening approach proposed by Methfessel and Paxton[32] is used with $N = 2$ and $\sigma = 0.2$ eV.

3. Results

3.1. Density Functional Theory (DFT) Calculations. We have investigated the ethylene/Rh(100) system with DFT calculations by computing the relative stabilities of all C_xH_y fragments in all conceivable adsorption sites (top, bridge, and hollow) with respect to chemisorbed ethylene (see Figure 1). Note that we have modeled the rhodium(100) surface within the slab model approximation using a four-metal layer slab model, describing a p(2 × 2) unit cell. The structures in Figure 1 therefore only represent a fraction of the actual slab size that was used. A comparison of the stabilities of the C_xH_y fragments on several metals, including rhodium, palladium, and platinum will be published elsewhere.[33] In order to compare these calculations with experiments, it is important to note that the DFT calculations were done on a (2 × 2) unit cell, such that the effective ethylene coverage is 0.25 monolayer.

To calculate the relative stabilities of the C_xH_y fragments, we have used the adsorption energy of ethylene in the di−σ geometry as a reference, with respect to which we have calculated a stabilization energy (or relative energy) of the fragment. Then, we have added the stabilization energy to the adsorption energy of ethylene in the di−σ geometry, and we have thus obtained an adsorption energy for the hydrocarbon fragment, which is meaningful and fully comparable to the adsorption energy of the ethylene molecule. Following this procedure we have built up an energy profile for the adsorption and decomposition of ethylene on Rh(100). This energy profile is self-explanatory and contains all the information we need in order to know which hydrocarbon fragments are energetically more stable and how strongly these are bound to the surface relative to adsorbed ethylene.

For example, if we want to calculate the adsorption energy of ethylidyne at a 4-fold hollow site, the "reaction" is as follows: C_2H_4 (di−σ) + slab → CCH_3 (hollow) + H (hollow). We now first need to calculate the stabilization energy of ethylidyne in the hollow site with respect to the ethylene molecule chemisorbed in the di−σ geometry:

$$\Delta E^{\mathrm{rel}}_{\mathrm{hollow}}(CCH_3) = E_{\mathrm{hollow}}(CCH_3) + E_{\mathrm{hollow}}(H) - E_{\mathrm{di}-\sigma}(C_2H_4) - E_{\mathrm{slab}}$$

in which E_{hollow} (CCH_3) and E_{hollow} (H) are the total energy of ethylidyne and atomic hydrogen at a 4-fold hollow site, respectively, $E_{\mathrm{di}-\sigma}$ (C_2H_4) is the total energy of ethylene adsorbed in a di−σ geometry, and E_{slab} is the total energy of the empty rhodium slab. Then, we sum up the resulting stabilization energy with the adsorption energy of the ethylene molecule in the di−σ geometry, and we obtain the adsorption energy of ethylidyne at a 4-fold hollow site:

$$\Delta E^{\mathrm{ads}}_{\mathrm{hollow}}(CCH_3) = \Delta E^{\mathrm{ads}}_{\mathrm{di}-\sigma}(C_2H_4) + \Delta E^{\mathrm{rel}}_{\mathrm{hollow}}(CCH_3)$$

The calculations show that only a few species are more stable than the adsorbed ethylene itself, notably ethylidyne (CCH_3) in a hollow site (0.61 eV more stable than molecularly adsorbed ethylene), acetylene (CHCH) in a hollow site (0.74 eV more stable), ethynyl (CCH) in a "bent" position (0.59 eV more stable), methylidyne (CH) in a hollow site (0.60 eV more stable), and carbon in a hollow site (0.62 eV more stable). From these calculations we expect that ethylene does not remain molecularly adsorbed but will decompose into (a mixture of) these species.

3.2. Temperature-Programmed Desorption (TPD) of H_2. The aim of the TPD experiments is to establish the decomposition pathway of ethylene by examining the hydrogen evolution. Hydrogen is the only product desorbing from the surface up to the ethylene saturation exposure. At exposures exceeding the saturation coverage, ethylene and a very small trace of ethane are also seen. Ethylene is then probably desorbing from a physisorbed or multilayer state, and a very small fraction hydrogenates to ethane. Figure 2 shows the hydrogen desorption traces, obtained after exposing the surface to ethylene at 90 K. For comparison, we also show the H_2 TPD spectra from the hydrocarbon-free Rh(100) surface. There are several desorption states for hydrogen, resulting in a complex desorption spectrum.

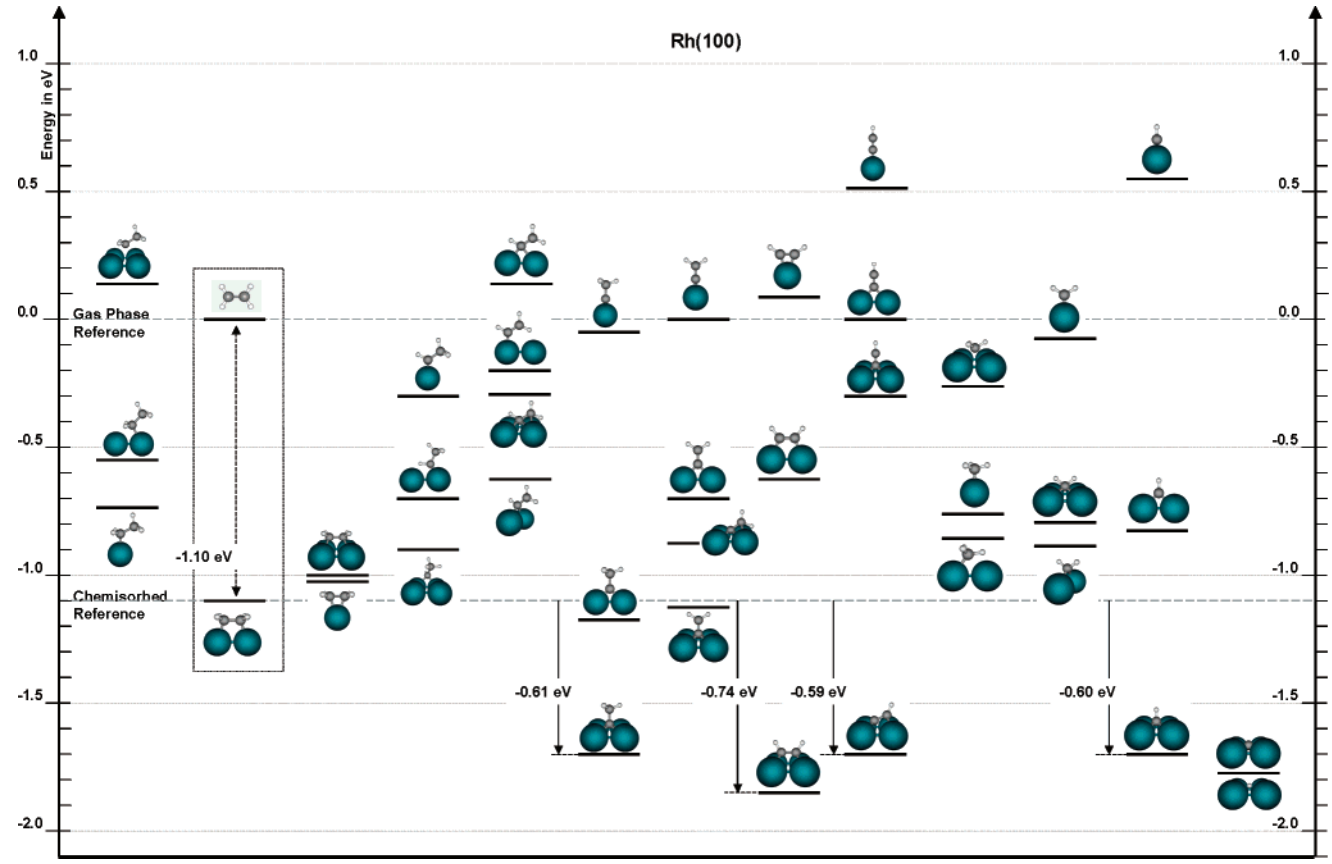

Figure 1. Energy profile of all possible C_xH_y fragments in all possible adsorption sites on the Rh(100) surface, according to DFT calculations (see Curulla Ferre et al.[33] for a comparison with other metals). Note that we have modeled the rhodium(100) surface within the slab model approximation using a four-metal layer slab model, describing a p(2 × 2) unit cell. The structures in Figure 1 therefore only represent a fraction of the actual slab size that was used. In principle, all the species below the chemisorbed reference are more stable than adsorbed ethylene. The numbers in the profile represent the additional "stabilization energy" relative to the adsorbed ethylene. A high negative number indicates that the species is much more stable on the surface than the adsorbed ethylene. There are five species more stable than molecularly adsorbed ethylene. Therefore, ethylene will probably not remain molecularly adsorbed but will decompose into (a mixture of) these products.

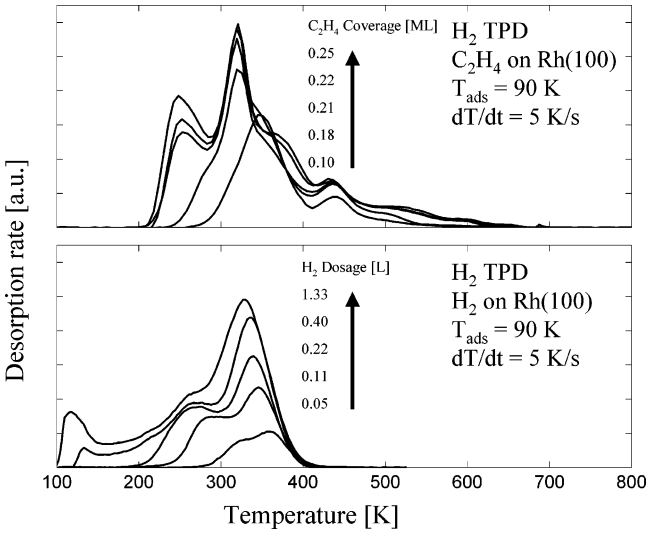

Figure 2. Temperature-programmed desorption (TPD) spectra of H_2 ($m/z = 2$) obtained after exposing the Rh(100) surface to various doses of C_2H_4 at 90 K (top) and H_2 at 90 K (bottom). The heating rate in both cases was 5 K/s. The coverage for ethylene is in monolayer [ML], and the dosage for hydrogen is in Langmuir [L].

At low coverage, the normal H_2 desorption spectrum (Figure 2, bottom) shows a desorption state at 360 K. At higher coverage, this state shifts and splits in two desorption states, one at 250 K and one at 330 K. These two states are also present in the H_2 spectrum resulting from ethylene decomposition (Figure 2, top). In addition, there are two clearly distinguishable decomposition-limited desorption states at 365 K and one at 440 K. There is still hydrogen evolution from the hydrocarbon layer in the temperature range from 440 K till 650 K. However, this does not occur in clearly structured peaks.

3.3. Static Secondary Ion Mass Spectrometry (SSIMS). Static SIMS has been performed to study the nature of the intermediate hydrocarbon species on the surface during the decomposition process. Figure 3 shows SSIMS spectra of the Rh(100) surface exposed to a low (0.10 ML) and a high (0.25 ML) dose of ethylene at 90 K and measured at 90 K. In addition, the spectrum of adsorbed ethylene heated to 600 K is included. All spectra have been normalized with respect to the $(Rh_2)^+$ peak intensity so that the figures represent in fact the intensity ratios $(Rh_2C_xH_y)^+/(Rh_2)^+$. These are generally semiquantitative indicators of coverage.[5,34−37] Seven distinct peaks appear in the mass range shown: $(Rh_2)^+$ at $m/z = 206$, $(Rh_2H)^+$ at $m/z = 207$, $(Rh_2C)^+$ at $m/z = 218$, $(Rh_2C_2)^+$ at $m/z = 230$, $(Rh_2C_2H)^+$ at $m/z = 231$, $(Rh_2C_2H_2)^+$ at $m/z = 232$, and $(Rh_2C_2H_3)^+$ at $m/z = 233$.

The low-coverage SSIMS spectrum (0.10 ML of C_2H_4) is dominated by the Rh_2C^+ and $Rh_2C_2H^+$ signals, consistent with the presence of C-atoms and CCH species. The spectrum at high coverage (0.25 ML) contains additional signals due to $Rh_2C_2H_2^+$ and $Rh_2C_2H_3^+$, indicating that more hydrogen-rich species such as acetylene and ethylidyne are present as well. The strong Rh_2H^+ signal is characteristic for adsorbed hydrogen, although a minor part of its intensity will be due to cracking of

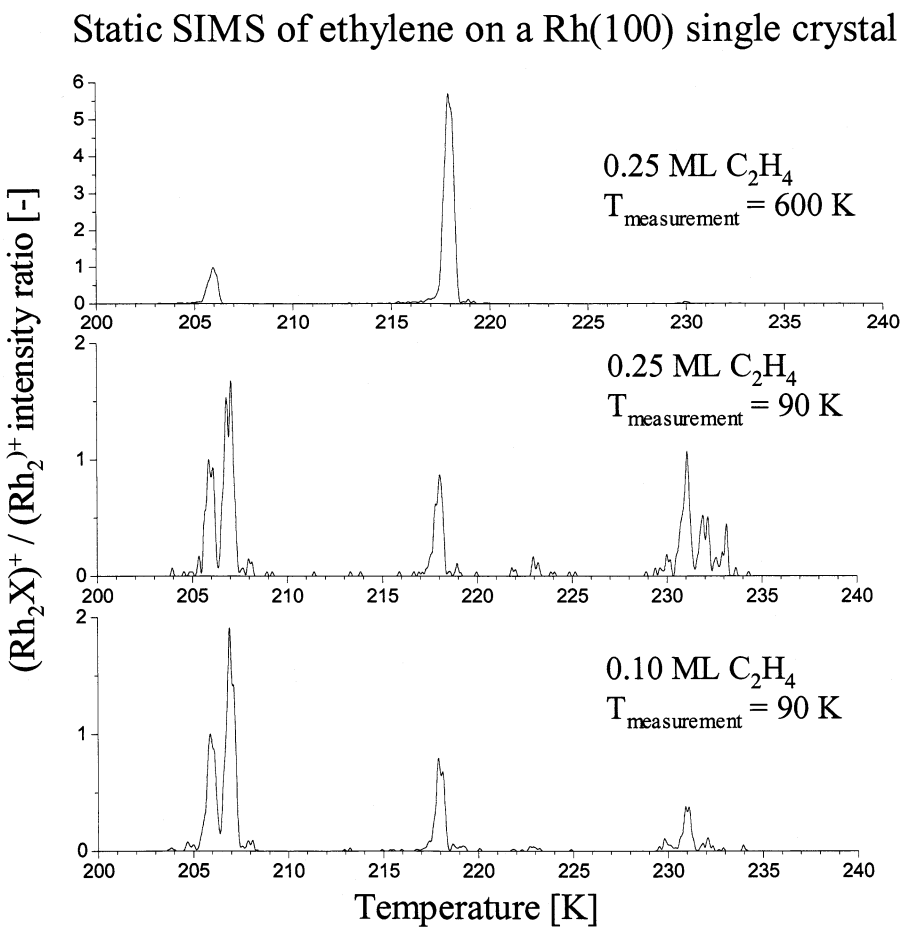

Figure 3. Static secondary ion mass spectrometry (SSIMS) spectra obtained after exposing the Rh(100) surface to 0.25 ML of ethylene (top) and (middle) and 0.10 ML of ethylene (bottom) at 90 K. The spectra were recorded at 600 K (top) and 90 K (bottom) and (middle).

secondary ions of the $Rh_2C_xH_y^+$ species. The spectrum obtained after heating to 600 K only shows the signal of Rh_2C^+, indicating that the hydrocarbon fragments have fully decomposed to atomic carbon. All the mass channels mentioned above are monitored in the temperature-programmed experiments that we describe next.

3.4. Temperature-Programmed Static Secondary Ion Mass Spectrometry (TPSSIMS). Figure 4 shows the temperature-programmed SSIMS traces of the species present on the surface during the decomposition process. In these experiments, the surface was exposed to ethylene at 90 K and subsequently heated at 5 K/s to 800 K. Again, we have plotted the intensity ratios $Rh_2C_xH_y^+/Rh_2^+$, which are at least qualitatively representative for the surface coverage of the intermediates. In addition, we show the H_2 desorption traces from the TPD spectra with the same initial coverage of ethylene. In brief, the experiments illustrate how ethylene at low coverages decays rapidly to ethynyl (CCH), which between 350 and 450 K converts to C-atoms**.** At higher coverage, larger species such as C_2H_2 and C_2H_3 appear at temperatures up to about 300 K, while between 300 and 500 K C_2H is the dominant species. Note that the conversion of C_2H to atomic carbon begins at lower temperature and is completed at higher temperatures than in the case of low ethylene coverage. Hence, ethylene decomposition proceeds at a slower rate at higher ethylene coverages, indicative of lateral interactions and site-blocking effects.

3.5. High-Resolution Electron Energy Loss Spectroscopy (HREELS). Figure 5 (top) shows the HREELS spectrum for low coverage of ethylene (0.10 ML). In this experiment the surface was exposed to ethylene at temperatures below 100 K and subsequently annealed to the indicated temperature. The surface was then cooled again, and the spectrum recorded at 100 K. Figure 5 (bottom) shows the HREELS spectrum for a saturation coverage of ethylene (0.25 ML). Assignment of the HREELS peaks was done mainly based on previous publications of Egawa,[8] Slavin et al.,[6,7] and Ibach and Lehwald[9] The assignments are summarized in Table 1.

The two most intense features are the ones at 940−960 cm^{-1}, which correspond to the ν(CC) stretch mode according to Egawa[8] and the peak at 2900−2920 cm^{-1}, which corresponds to the $\nu(CH_3)$ stretch mode according to Slavin et al.[6] Furthermore, there are peaks at 3070−3090 cm^{-1} (ν(CH) stretch mode) and 820−840 cm^{-1} (δ(CH) bend mode) (Slavin et al.[6] and Egawa[8]).

3.6. Low-Energy Electron Diffraction (LEED). Figure 6 shows the LEED pattern for a saturation dosage of ethylene at 90 K. Ethylene is ordered in a p(2 × 2) pattern, corresponding to a saturation coverage of 0.25 ML. However, this LEED pattern only exists at low temperature. Upon increasing the temperature the pattern changes to a c(2 × 2) pattern formed by the carbon overlayer.

4. Discussion

Before we discuss the results in detail, we note that the present work illustrates how computational and experimental approaches have integrated in surface science anno 2004. It is nowadays easier to calculate how molecules adsorb and decompose than

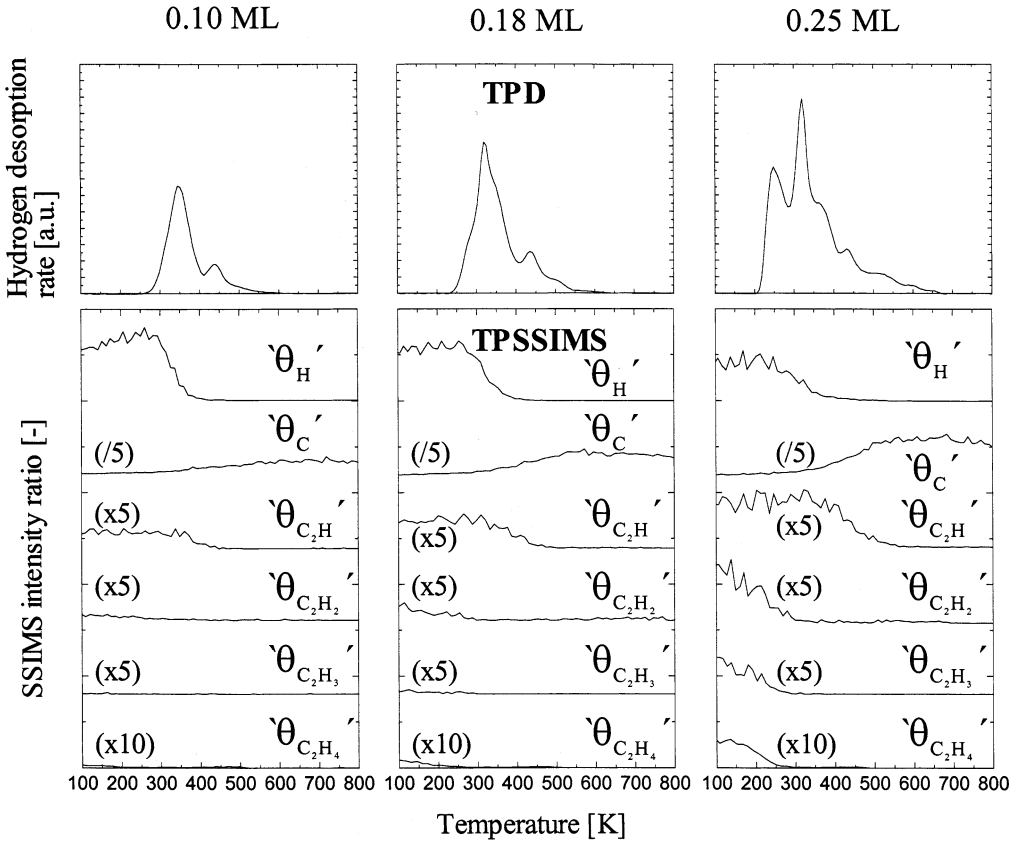

Figure 4. Selected H_2 desorption traces from Figure 2 and $(Rh_2X)^+/(Rh_2)^+$ temperature-programmed static SIMS ion intensity ratios, representing the surface coverages of the decomposition products, during temperature-programmed decomposition of ethylene on Rh(100), for low (left panel), medium (middle panel), and high (right panel) initial ethylene coverages.

to measure it. Verification of computational results, however, remains essential before we can fully rely on computational chemistry. The present study of ethylene decomposition on Rh(100) reveals that the predictions from DFT are in remarkable agreement with the experiments: particularly the static SIMS results contain evidence for all the stable fragments in the calculations, whereas HREELS confirms the presence of ethylidyne on Rh(100) and supports the presence of CCH and possibly CH species. Nevertheless, it is important to be aware of shortcomings in both the experimental and theoretical approach. In spectroscopy we may not be able to observe all species due to selection rules in vibrational spectroscopy, or due to stability issues in secondary ion mass spectrometry, or simply because the surface concentration is too low. In computational chemistry we may have overlooked certain species, simply because we did not consider them in the calculation. Furthermore, the accuracy and flexibility of the simulations is still limited, and parameters such as number of *k*-points and depth of the slab model need to be chosen carefully in order to obtain meaningful results. So, whereas both experiment and theory have their pros and cons, it is often the combination of both methods that proves to be a powerful tool in unraveling a catalytic process.

Following is a detailed discussion of the results.

4.1. Low Ethylene Coverage (0.10 ML). In brief, ethylene at coverages around 0.10 ML decomposes rapidly to ethynyl (CCH), which is the dominant species at 90 K and is stable up to about 350 K, where it starts to decay (Figure 4). The SSIMS spectrum shows that at 90 K mainly ethynyl is present, next to very small amounts of acetylene, while ethylidyne is absent. The HREELS spectrum (Figure 5) indicates a small peak at 2918 cm^{-1} (characteristic for the CH_3 stretch mode[6]) for temperatures below 100 K. Upon increasing the temperature above 100 K, the peak for the CH_3 stretch mode vanishes and peaks corresponding to the ethynyl species appear: 3070−3090 cm^{-1} and 820−840 cm^{-1}, corresponding to the CH stretch and bend mode, respectively. So, above 100 K both methods confirm that ethynyl is the main species on the surface. The HREELS and SSIMS spectra contradict each other only at the lowest temperature: the HREELS spectrum suggests the presence of a CCH_3 species and the SSIMS spectrum mainly a CCH species. The reason for the discrepancy at temperatures below 100 K is in our view due to the presence of the contaminant CO in the HREELS experiment. As can be seen from Figure 5 (top), there are peaks at 280 and 2198 cm^{-1} for the spectrum below 100 K, which are attributed to a small amount of physisorbed CO. This CO might slightly slow down or hinder the decomposition process. This was also observed by Slavin et al.,[7] who were able to produce only the CCH_3 intermediate by coadsorbing CO and ethylene. The CO has desorbed in the second HREELS spectrum at 200 K, and there also the CCH_3 peak has disappeared. Only the HREELS experiment suffers from this CO due to the nature of the HREELS setup and experiment, which involves a slightly longer time period between sample cleaning and actual experiment. During this time period, a small amount of CO (which was used during the cleaning procedure) has apparently physisorbed onto the surface. In the SSIMS experiment the time period between cleaning the sample and measuring was smaller. Therefore, in this experiment no CO was detected and no inhibition of ethylene decomposition was observed.

Upon increasing the temperature, the hydrogen and carbon content on the surface remain more or less constant till 300 K. The TPD spectrum shows that above 300 K hydrogen starts to desorb from the surface. This hydrogen desorption creates vacant sites on the surface, enabling the further decomposition of the

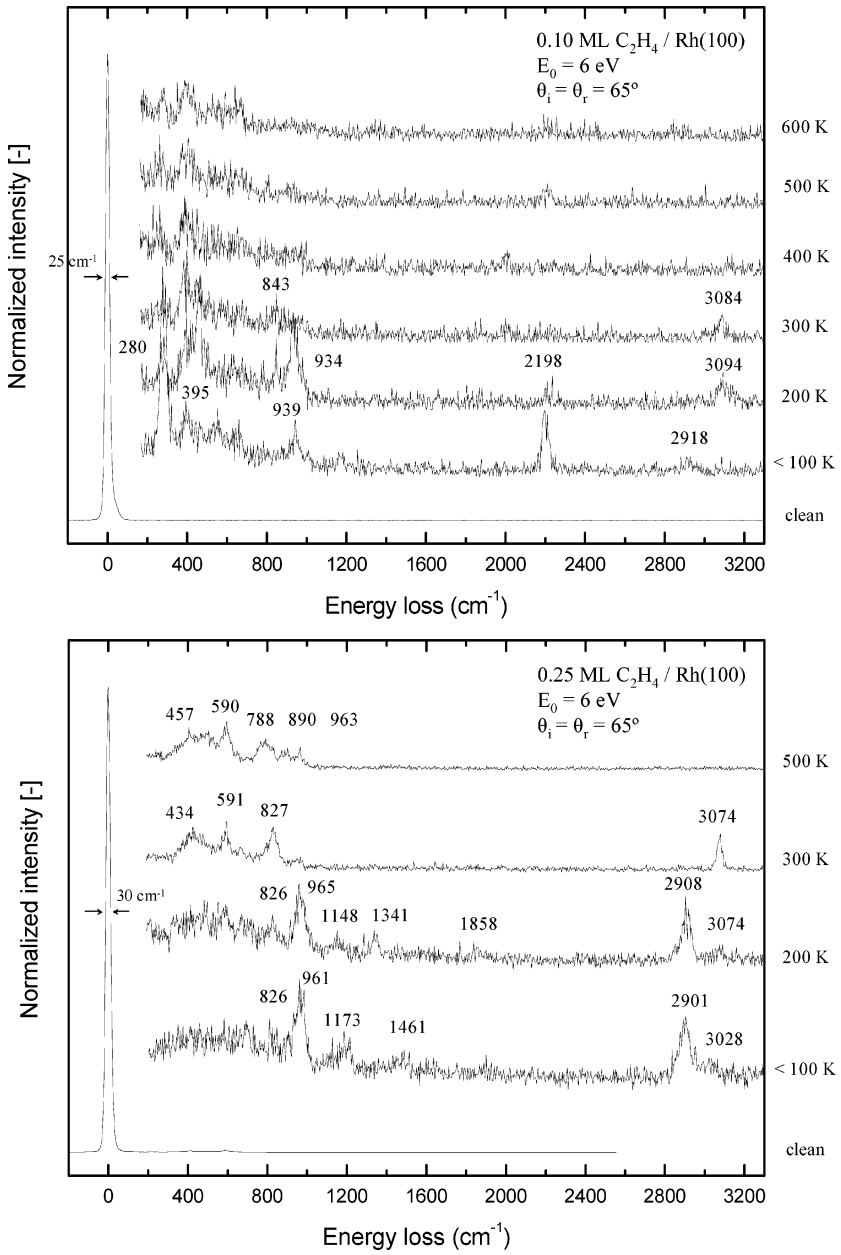

Figure 5. High-resolution electron energy loss spectroscopy (HREELS) spectra of ethylene on Rh(100) for a low coverage (0.10 ML) (top) and a saturation coverage (0.25 ML) of ethylene (bottom). Ethylene was adsorbed below 100 K. The surface was then flashed till the indicated temperature, and the spectra were recorded at 100 K. All spectra have been normalized with respect to the elastic peak.

TABLE 1: Assignments of Vibrational Frequencies (cm^{-1}) of Ethylene on Rh(100)[a]

mode assignment	Rh(100)/ 0.10 ML C_2H_4	Rh(100)/ 0.25 ML C_2H_4
ν(CH)	~3090	~3070
$\nu(CH_3)$	~2920	~2900
ν(CC)	~940	~960
δ(CH)	~840	~820
$\nu(Me-C_xH_y)$	~400	~400
ν(CO)		~1860
$\nu(CO_{physisorbed})$	~2200	
$\nu(Me-CO_{physisorbed})$	~280	

[a] Assignment was done mainly based on previous publications of Egawa,[8] Slavin et al.,[6,7] and Ibach and Lehwald.[9]

ethynyl species, which indeed starts after the main H_2 desorption peak around 350 K and is completed around 450 K. The HREELS confirms that between 400 and 500 K the ethynyl species is fully decomposed. The decomposition of ethynyl is accompanied by an increase in the carbon content on the surface.

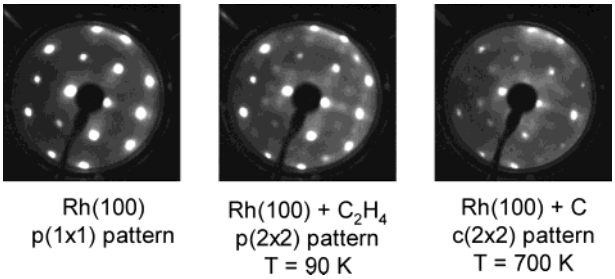

Figure 6. LEED images of clean Rh(100) (left), Rh(100) with a saturation layer of ethylene at 90 K (middle), and Rh(100) with a carbon layer formed by the decomposition of a saturation layer of ethylene (right). A saturation layer of ethylene results in a p(2 × 2) pattern, corresponding to a coverage of 0.25 ML. Upon increasing the temperature, ethylene decomposes into carbon and hydrogen. The resulting carbon layer on the surface is ordered in a c(2 × 2) fashion.

Above 450 K all ethynyl has been decomposed. However, as H_2 evolution occurs up to 550 K, we suggest that CH is the

dominant species between 450 and 550 K and C-atoms at higher temperature. In brief:

$$\underset{\text{ethylene}}{C_2H_4} \xrightarrow{90\ \text{K}} \underset{\text{ethynyl}}{C_2H} \xrightarrow{350-450\ \text{K}} \underset{\text{methylidyne}}{CH} \xrightarrow{450-550\ \text{K}} \underset{\text{C-atoms}}{C}$$

4.2. High Ethylene Coverage (0.25 ML). The decomposition of ethylene at higher coverages on Rh(100) is slowed down, due to a combination of lateral interactions between adsorbed species and site-blocking effects. The TPSSIMS spectra in Figure 4 show that there is some decomposition of ethylene already at low temperatures (below 100 K), since hydrogen and decomposition products are present on the surface. The hydrogen level is significantly higher than what could be expected from background adsorption. According to Figure 3, there are three different hydrocarbon fragments present on the surface next to molecular ethylene: these are C_2H_3, C_2H_2, and C_2H. All are among the stable species of the computational scheme of Figure 1. A small fraction of these species may be sensitive to cracking in the mass spectrometer. However, the C_2H_3, C_2H_2, and C_2H fragments show an intensity of the same order of magnitude; hence, we believe that the species are indeed present on the surface. The HREELS spectrum shows the $\nu(CH_3)$ stretch mode and the ν(CC) stretch mode, in agreement with the presence of the ethylidyne species. Furthermore, small signals for the δ-(CH) bend mode and the ν(CH) stretch mode are present, in agreement with the ethynyl species. In addition, the TPSSIMS spectrum suggests that there is also molecular ethylene on the surface. One has to be careful in directly comparing the intensities for static SIMS and HREELS. Both methods have different detection sensitivities toward different fragments. Therefore, a high signal in one method need not be accompanied by a high signal in the other method. The presence of a signal in both methods, however, is a strong indication of the presence of the fragment on the surface. Therefore, we conclude that at low temperatures, a mixture of molecular ethylene, ethylidyne, acetylene, and ethynyl together with hydrogen and carbon is present on the surface.

The carbon signal in TPSSIMS (see Figure 4), although somewhat sensitive to decomposition of higher fragments in the mass spectrometer, can be taken as a measure of the decomposition that has occurred, and this signal is still very low at a temperature below 100 K. Upon increasing the temperature to 300 K, ethylene, ethylidyne, and acetylene decompose. This is accompanied by a slight increase in the carbon signal. The ethynyl species, however, is very stable and does not decompose yet. Note that there is no hydrogen desorption from ethylene below 200 K according to the TPD spectra. Since only the low-coverage spectra of normal H_2 desorption also show no desorption below 200 K, this could indicate that the hydrogen coverage is quite low. Nevertheless, ethylene does not remain fully molecularly adsorbed below 200 K (Slavin et al.[6]), but decomposes to some extent. The TPD spectrum shows that above 200 K hydrogen starts to desorb from the surface, while the SIMS signal for hydrogen decreases from 250 K onward. This indicates that for a short temperature range (between 200 and 250 K) the amount of hydrogen on the surface remains more or less constant, indicating an equilibrium between the amount of hydrogen produced by the decomposition of ethylene, ethylidyne, and acetylene and the amount of hydrogen desorbing. Note that the onset of the decrease of the hydrogen concentration on the surface (at 250 K) is about 50 K lower than for the low-coverage case, indicative of lateral interactions.

The TPSSIMS spectrum shows that at room temperature, 300 K, ethylene, ethylidyne, and acetylene are no longer present on the surface. The HREELS spectrum confirms that the ethylidyne species has been decomposed, since the $\nu(CH_3)$ stretch mode has disappeared. At this temperature the HREELS spectrum only shows the δ(CH) bend mode and the ν(CH) stretch mode. This is consistent with the SIMS spectrum which also indicates that only ethynyl is present on the surface, next to carbon and hydrogen. The HREELS spectrum only shows a small signal for the ν(CC) stretch mode, but since the ethynyl is most likely present in a "bent" mode parallel to the surface, according to the DFT calculations, we can expect the signal to be weak in a specular HREELS measurement.

Above 250 K, the rate of hydrogen removal from the surface is higher than the rate of production. Therefore the hydrogen coverage of the surface decreases as seen in the SIMS data (Figure 4), creating vacant sites on the surface. This enables the decomposition of ethynyl (C_2H), which starts around 300 K as shown by the temperature-programmed SIMS data (Figure 4). The decrease of the ethynyl coverage is accompanied by an increase in the carbon coverage. It takes till 500 K before all ethynyl has been converted. Note that at a high initial ethylene coverage the ethynyl species starts decomposing at a temperature that is 50 K lower and is fully decomposed at a temperature that is 50 K higher compared to the low-coverage case. This indicates that the decomposition process is slowed down at higher coverages. Above 500 K most of the hydrogen has left the surface, while carbon remains on the surface, as shown by the SIMS spectra. The HREELS spectrum confirms the decomposition of ethynyl since the peaks indicating the CH bend and stretch modes have almost disappeared at 500 K. There are still some poorly resolved desorption states for hydrogen above 500 K in the TPD spectrum, which are probably due to small amounts of methylidyne that are still present on the surface. Above 700 K there is no hydrogen desorption anymore. Carbon is strongly bound to the surface and does not desorb but can diffuse into the bulk at higher temperatures. Note that the final, total carbon content on the surface is much higher than for the low-coverage case (see Figure 4). In brief:

$$\underset{\text{ethylene}}{C_2H_4} \xrightarrow{100-300\ \text{K}} \underset{\text{ethylidyne/acetylene}}{C_2H_3/C_2H_2} \xrightarrow{100-300\ \text{K}} \underset{\text{ethynyl}}{C_2H}$$

$$\underset{\text{ethylene}}{C_2H_4} \xrightarrow{100-300\ \text{K}} \underset{\text{ethynyl}}{C_2H}$$

$$\underset{\text{ethynyl}}{C_2H} \xrightarrow{300-500\ \text{K}} \underset{\text{methylidyne}}{CH} \xrightarrow{500-700\ \text{K}} \underset{\text{C-atoms}}{C}$$

4.3. Hydrogen Desorption States. In principle there are four desorption states for hydrogen. In addition to the two desorption states in a normal H_2 desorption spectra from a hydrocarbon-free surface (peaks at 250 and 330 K), the H_2 desorption trace from ethylene decomposition shows two extra, decomposition-limited, states at 365 and 440 K. The peak at 440 K can be attributed to the decomposition of the ethynyl species. This is shown very clearly by the TPSSIMS spectrum for the 0.10 ML ethylene coverage (Figure 4, left panel). The only species on the surface here is the ethynyl, and the temperature of its decomposition coincides with the hydrogen desorption peak at 440 K in Figure 2.

For a high initial ethylene coverage, both decomposition-limited H_2 desorption peaks are present. Slavin et al.[6] assigned the peak at 365 K to the conversion of ethylidyne to acetylene with subsequent conversion to ethynyl. We find that both

ethylidyne and acetylene are already converted at 300 K, below the desorption state of 365 K. Hence we attribute the H_2 evolution at 365 K directly to the formation of the ethynyl (CCH) fragment from ethylidyne and acetylene.

5. Conclusions

Density functional calculations of ethylene-derived hydrocarbon fragments adsorbed on the (100) surface of rhodium predict the following species to be stable: ethylene itself, ethylidyne (CCH_3) in a hollow site, acetylene (CHCH) in a hollow site, ethynyl (CCH) in a "bent" position with each carbon bound to two rhodium atoms, methylidyne (CH) in a hollow site, and carbon in a hollow site. Spectroscopic confirmation of these species has been obtained from high-resolution electron energy loss spectroscopy and static secondary ion mass spectrometry, and in an indirect way via temperature-programmed desorption of hydrogen. Low-energy electron diffraction shows that a saturation layer of ethylene orders in a p(2 × 2) structure, implying a saturation coverage of 0.25 ML for the ethylene. The resulting carbon layer after complete decomposition orders in a c(2 × 2) fashion. Temperature-programmed SIMS and temperature-programmed desorption give insight into the stability ranges of the species. The nature and rate of decomposition of the hydrocarbon fragments depends on the surface coverage. Ethynyl (CCH) and methylidyne (CH) are the dominant intermediates in the decomposition of ethylene to carbon at low coverage, whereas ethylidyne (CCH_3) and acetylene (CHCH) appear as stable intermediates at saturation coverage. The rate of decomposition is highest at low coverage.

Acknowledgment. The authors gratefully acknowledge financial support by The Netherlands Organization for Scientific Research (NWO) through Grant 700-50-012 and by the National Computing Facilities Foundation (NCF) through Grant MP-072-A. The work was carried out under the auspices of The Netherlands Institute for Catalysis Research (NIOK).

References and Notes

(1) Borg, H. J.; Hardeveld, R. M. v.; Niemantsverdriet, J. W. *J. Chem. Soc., Faraday Trans.* **1995**, *91*, 3679.
(2) Somorjai, G. A.; Van Hove, M. A.; Bent, B. E. *J. Phys. Chem.* **1988**, *92*, 973.
(3) Dubois, L. H.; Castner, D. G.; Somorjai, G. A. *J. Chem. Phys.* **1980**, *72*, 5234.
(4) Zaera, F. *J. Am. Chem. Soc.* **1989**, *111*, 8744.
(5) Lauderback, L. L.; Delgass, W. N. *ACS Symp. Ser.* **1984**, *248*, 21−37.
(6) Slavin, A. J.; Bent, B. E.; Kao, C.-T.; Somorjai, G. A. *Surf. Sci.* **1988**, *206*, 124−144.
(7) Slavin, A. J.; Bent, B. E.; Kao, C.-T.; Somorjai, G. A. *Surf. Sci.* **1988**, *202*, 388−404.
(8) Egawa, C. *Surf. Sci.* **2000**, *454*−*456*, 222−226.
(9) Ibach, H.; Lehwald, S. *J. Vac. Sci. Technol.* **1978**, *15*, 407−415.
(10) Bent, B. E.; Mate, C. M.; Kao, C.-T.; Slavin, A. J.; Somorjai, G. A. *J. Phys. Chem.* **1988**, *92*, 4720−4726.
(11) Stuve, E. M.; Madix, R. J.; Brundle, C. R. *Surf. Sci.* **1985**, *152*−*153*, 532−542.
(12) Stuve, E. M.; Madix, R. J. *J. Phys. Chem.* **1985**, *89*, 105−112.
(13) Zaera, F.; Hall, R. B. *Surf. Sci.* **1987**, *180*, 1−18.
(14) Zaera, F.; Hall, R. B. *J. Phys. Chem.* **1987**, *91*, 4318−4323.
(15) Zhu, X. Y.; Castro, M. E.; Akhter, S.; White, J. M.; Houston, J. E. *J. Vac. Sci. Technol., A* **1989**, *7*, 1991−1995.
(16) Hardeveld, R. M. v.; Schmidt, A. J. G. W.; Santen, R. A. v.; Niemantsverdriet, J. W. *J. Vac. Sci. Technol., A* **1997**, *15*, 1642−1646.
(17) Hardeveld, R. M. v.; Santen, R. A. v.; Niemantsverdriet, J. W. *J. Phys. Chem. B* **1997**, *101*, 7901−7907.
(18) Hardeveld, R. M. v.; Schmidt, A. J. G. W.; Niemantsverdriet, J. W. *Catal. Lett.* **1996**, *41*, 125−131.
(19) Koestner, R. J.; Van Hove, M. A.; Somorjai, G. A. *Surf. Sci.* **1982**, *121*, 321.
(20) Wander, A.; Van Hove, M. A.; Somorjai, G. A. *Phys. Rev. Lett.* **1991**, *67*, 626.
(21) Levis, R.; Winograd, N. *J. Am. Chem. Soc.* **1987**, *109*, 6873.
(22) Linke, R.; Curulla, D.; Hopstaken, M. J. P.; Niemantsverdriet, J. W. *J. Chem. Phys.* **2001**, *115*, 8209−8216.
(23) Niemantsverdriet, J. W. *Spectroscopy in Catalysis*, 2nd ed.; Wiley-VCH: Weinheim, 2000.
(24) Castner, D. G.; Somorjai, G. A. *Surf. Sci.* **1979**, *83*, 60−82.
(25) Singh, H. P. *Acta Crystallogr., Sect. A* **1968**, *24*, 469.
(26) Kresse, G.; Hafner, J. *Phys. Rev. B: Condens. Matter* **1993**, *47*, 558.
(27) Kresse, G.; Furthmüller, J. *Phys. Rev. B: Condens. Matter* **1996**, *54*, 11169.
(28) Wang, Y.; Perdew, J. P. *Phys. Rev. B: Condens. Matter* **1991**, *44*, 13298.
(29) Perdew, J. P.; Chevary, J. A.; Vosko, S. H.; Jackson, K. A.; Pederson, M. R.; Singh, D. J.; Fiolhais, C. *Phys. Rev. B: Condens. Matter* **1992**, *46*, 6671.
(30) Vanderbilt, D. *Phys. Rev. B: Condens. Matter* **1990**, *41*, 7892.
(31) Monkhorst, H. J.; Pack, J. D. *Phys. Rev. B: Condens. Matter* **1976**, *13*, 5188.
(32) Methfessel, M.; Paxton, A. T. *Phys. Rev. B: Condens. Matter* **1989**, *40*, 3616.
(33) Curulla Ferre, D., Nieskens, D. L. S.; Niemantsverdriet, J. W., submitted for publication, 2004.
(34) Zhu, X. Y.; White, J. M. *J. Phys. Chem.* **1988**, *92*, 3970.
(35) Borg, H. J.; Niemantsverdriet, J. W. *Catalysis* **1994**, *11*, 1.
(36) Briggs, D.; Brown, A.; Vickerman, J. C. *Handbook of Static Secondary Ion Mass Spectrometry*; Wiley: Chichester, 1989.
(37) Benninghoven, A.; Beckmann, P.; Greifendorf, D.; Muller, K.-H.; Schemmer, M. *Surf. Sci.* **1981**, *107*, 148−164.